The Journal of Comparative Neurology 515:243–259 (2009)
Research in Systems Neuroscience

Total Number and Volume of Von Economo Neurons in the Cerebral Cortex of Cetaceans

CAMILLA BUTTI,[1,2] CHET C. SHERWOOD,[3] ATIYA Y. HAKEEM,[4] JOHN M. ALLMAN,[4] AND PATRICK R. HOF[1,5]*

[1]Department of Neuroscience, Mount Sinai School of Medicine, New York, New York 10029
[2]Department of Experimental Veterinary Sciences, University of Padova, Padova, Italy I-35131
[3]Department of Anthropology, George Washington University, Washington, DC 20052
[4]Division of Biology, California Institute of Technology, Pasadena, California 91125
[5]New York Consortium in Evolutionary Primatology, New York, New York

ABSTRACT

Von Economo neurons (VENs) are a type of large, layer V spindle-shaped neurons that were previously described in humans, great apes, elephants, and some large-brained cetaceans. Here we report the presence of Von Economo neurons in the anterior cingulate (ACC), anterior insular (AI), and frontopolar (FP) cortices of small odontocetes, including the bottlenose dolphin (*Tursiops truncatus*), the Risso's dolphin (*Grampus griseus*), and the beluga whale (*Delphinapterus leucas*). The total number and volume of VENs and the volume of neighboring layer V pyramidal neurons and layer VI fusiform neurons were obtained by using a design-based stereologic approach. Two humpback whale (*Megaptera novaeangliae*) brains were investigated for comparative purposes as representatives of the suborder Mysticeti. Our results show that the distribution of VENs in these cetacean species is comparable to that reported in humans, great apes, and elephants. The number of VENs in these cetaceans is also comparable to data available from great apes, and stereologic estimates indicate that VEN volume follows in these cetacean species a pattern similar to that in hominids, the VENs being larger than neighboring layer V pyramidal cells and conspicuously larger than fusiform neurons of layer VI. The fact that VENs are found in species representative of both cetacean suborders in addition to hominids and elephants suggests that these particular neurons have appeared convergently in phylogenetically unrelated groups of mammals possibly under the influence of comparable selective pressures that influenced specifically the evolution of cortical domains involved in complex cognitive and social/emotional processes. J. Comp. Neurol. 515:243–259, 2009.

Indexing terms: cetaceans; cingulate cortex; insula; prefrontal cortex; stereology; Von Economo neurons

Cetaceans diverged from terrestrial mammals during the early Paleocene about 55 million years ago (Gingerich and Uhen, 1998; Gingerich et al., 2001) and from the ancestral group of mammals that led to modern primates about 90–95 million years ago (Bromham et al., 1999). From a phylogenetic point of view, cetaceans are included in a superorder, the cetartiodactyls, which groups them with all even-toed ungulates, the hippopotamids being their closest relatives on the grounds of molecular phylogenetics (Gatesy, 1997; Boisserie et al., 2005; Agnarsson and May-Collado, 2008). During their adaptation to aquatic life, however, cetaceans evolved large brains and an expanded neocortex with a high degree of gyrification compared to ungulates. The brains of cetaceans are very large in both absolute and relative size and possess encephalization quotients (EQ) that are second only to humans (Marino, 1998). At the gross morphological level, the cetacean brain is very different from the brain of anthropoid primates in terms of gyral and sulcal patterns, and this difference is even more obvious when considering cortical cytoarchitecture. The cetacean neocortex is characterized, in contrast to that of primates, by the presence of only five cortical layers: a very thick layer I that is far more cellular than in most terrestrial species; a densely packed layer II displaying cellular clustering in many cortical regions, particularly in the insula (Manger et al., 1998; Hof and Van der Gucht, 2007) and con-

Grant sponsor: The James S. McDonnell Foundation; Grant number: 22002078.

*Correspondence to: Patrick R. Hof, Department of Neuroscience, Box 1065, Mount Sinai School of Medicine, One Gustave L. Levy Place, New York, NY 10029. E-mail: patrick.hof@mssm.edu.

Received 7 October 2008; Revised 14 January 2009; Accepted 24 February 2009

DOI 10.1002/cne.22055

Published online March 20, 2009 in Wiley InterScience (www.interscience.wiley.com).

taining isolated, very large, inverted-pyramid-like neurons; a wide pyramidal layer III; a relatively thin pyramidal layer V containing large pyramidal cells usually distributed in small clusters; and a multiform layer VI (Morgane et al., 1988; Glezer and Morgane, 1990; Hof and Sherwood, 2005; Hof and Van der Gucht, 2007). This cortical lamination pattern with the lack of an internal granular layer IV may reflect a particular cortical wiring organization in cetaceans (Hof and Van der Gucht, 2007). Nonetheless, neocortical complexity, extreme gyrification, and large size (Oelschläger and Oelschläger, 2002; Hof et al., 2005; Hof and Van der Gucht, 2007) represent remarkable features of the cetacean brain.

Several hypotheses have been developed on the functional significance of such an increase in brain size and structural complexity in cetaceans, yet the adaptive pressures that conditioned this development are still a matter of debate (Manger, 2006; Marino et al., 2007, 2008). The anatomical features of cetacean brains are interesting in light of evidence of their sophisticated behavioral and cognitive abilities. In fact, cetaceans exhibit, both in the wild and in captivity, several cognitive convergences with primates and humans (Marino, 2002; Marino et al., 2007). Laboratory studies report strong evidence of declarative and procedural cognitive abilities as well as social knowledge and self-awareness in the bottlenose dolphin (for review see Marino et al., 2007). Complex social structures, long-term bonds, higher order alliances, cooperative networks, as well as possible cultural transmission and tool use have been documented in the wild in several cetacean species (for review see Krushinskaya, 1986; Marino et al., 2007, 2008), leading to questions about the nature of the evolution of cognition in groups of phylogenetically divergent mammals.

In this study, we focus on a particular neuronal type, the Von Economo neurons (VENs), that have been proposed to subserve certain aspects of higher cognitive abilities in humans such as social and emotional cognition, awareness, and intuition (Allman et al., 2005). VENs are large, bipolar projection neurons located in layer V of the anterior cingulate cortex (ACC) and frontoinsular cortex (FI) that were originally described in humans and great apes (Nimchinsky et al., 1995, 1999). VENs are more abundant in humans than in great apes (Allman et al., 2005, 2009) and are larger than neighboring pyramidal neurons and fusiform cells (Nimchinsky et al., 1999). Aside from hominids, VENs have been recently observed with a similar regional distribution in the elephant brain (Hakeem et al., 2009) and in the humpback whale (*Megaptera novaeangliae*), the fin whale (*Balaenoptera physalus*), the sperm whale (*Physeter macrocephalus*), and the killer whale (*Orcinus orca*; Hof and Van der Gucht, 2007). VEN-like, large spindle neurons occur in the neocortex of the harbor porpoise (*Phocoena phocoena*; Behrmann, 1993) and were considered a variant of the largest pyramidal cells.

Quantitative data on VENs in cetaceans, to complement studies in hominds and elephants, are lacking. We examined the brain of smaller odontocetes, including the bottlenose dolphin (*Tursiops truncatus*), the Risso's dolphin (*Grampus griseus*), and the beluga whale (*Delphinapterus leucas*), as well as two humpback whales (*M. novaeangliae*) as a representative of the suborder Mysticeti, for comparative purposes, in view of a recent observation that in the bottlenose dolphin, contrary to our previous report (Hof and Van der Gucht, 2007), VENs appear also to be present in the ACC, FI, and frontopolar cortex (FP) of small odontocetes (Hakeem et al., 2009). With these species and regions, we performed a quantitative study of the total number of VENs and their somatic volume in comparison with that of the neighboring layer V pyramidal neurons and layer VI fusiform neurons.

MATERIALS AND METHODS

Brain specimens and tissue processing

Five cetacean brains from specimens belonging to both toothed whales (Odontoceti, Delphinoidea: bottlenose dolphin, *T. truncatus*; Risso's dolphin, *G. griseus*; beluga whale, *D. leucas*) and baleen whales (Mysticeti, Balaenopteridae: humpback whale, *M. novaeangliae*) were examined in the present study (Fig. 1). The brains of a captive juvenile male bottlenose dolphin (1.90 m beak-to-fluke notch length, 3 years old) and of a stranded adult female Risso's dolphin (2.90 m beak-to-fluke notch length, 18 years old) were collected at necropsy within 24 hours from death, postfixed, and stored in 10% formalin for about 3 years at the Marine Mammals Tissue Bank of the University of Padova, Italy. Blocks of ACC from the left hemisphere and the right hemisphere, respectively, were collected, cryoprotected in graded sucrose solutions up to 30%, frozen in dry ice, and cut into 80-μm-thick coronal sections with a sliding microtome (Leica Biosystems, Nussloch, Germany). The sections were then mounted on glass slides, Nissl-stained in a 0.2% cresyl violet solution, and coverslipped in 70% DPX in xylene for examination. The brain of a female humpback whale (13.7 m beak-to-fluke notch length) was collected after stranding and postfixed in 10% formalin. Blocks containing the left ACC and the left anterior insula were collected and cut into serials 3-cm-thick slabs. These slabs were then processed as for the bottlenose dolphin's blocks. Blocks from the right ACC and anterior insula of a beluga whale and the whole right hemisphere of the brain of a stranded adult female humpback whale (13.8 m beak-to-fluke notch length) were dehydrated in graded alcohol solutions up to 30%, embedded in celloidin, and processed serially at 35 μm on a modified large-specimen microtome (Jacobs et al., 1971, 1979, 1984). The hemisphere of the humpback whale was cut in the sagittal plane relative to the beak-fluke axis, whereas the blocks from the beluga brain were cut into the coronal plane, and series of adjacent sections were selected for the quantitative analysis. Sections were stained alternatively for Nissl substance with the Bielchowsky-Plien cresyl violet method or for myelin with the Loyez-Weigert method (Bertrand, 1930). The sections were then mounted on glass slides and coverslipped in clarite for examination. The brains of the two humpbacks and of the beluga whale were collected in the 1960s and kept in fixative for an unknown amount of time. Information on the post-mortem interval was also not available for these three specimens. Unfortunately, we were not able to examine all the regions of interest (ROIs) in every species owing to the availability of the materials. In some cases, part of an ROI or a whole ROI was not collected or had been used by other investigators and thus was not available for the present study. Finally, because the brains of the specimens investigated in the present study were collected from different sources and information on the specific brain and body weight were not available, average values from the literature for each of these species are provided in Table 1.

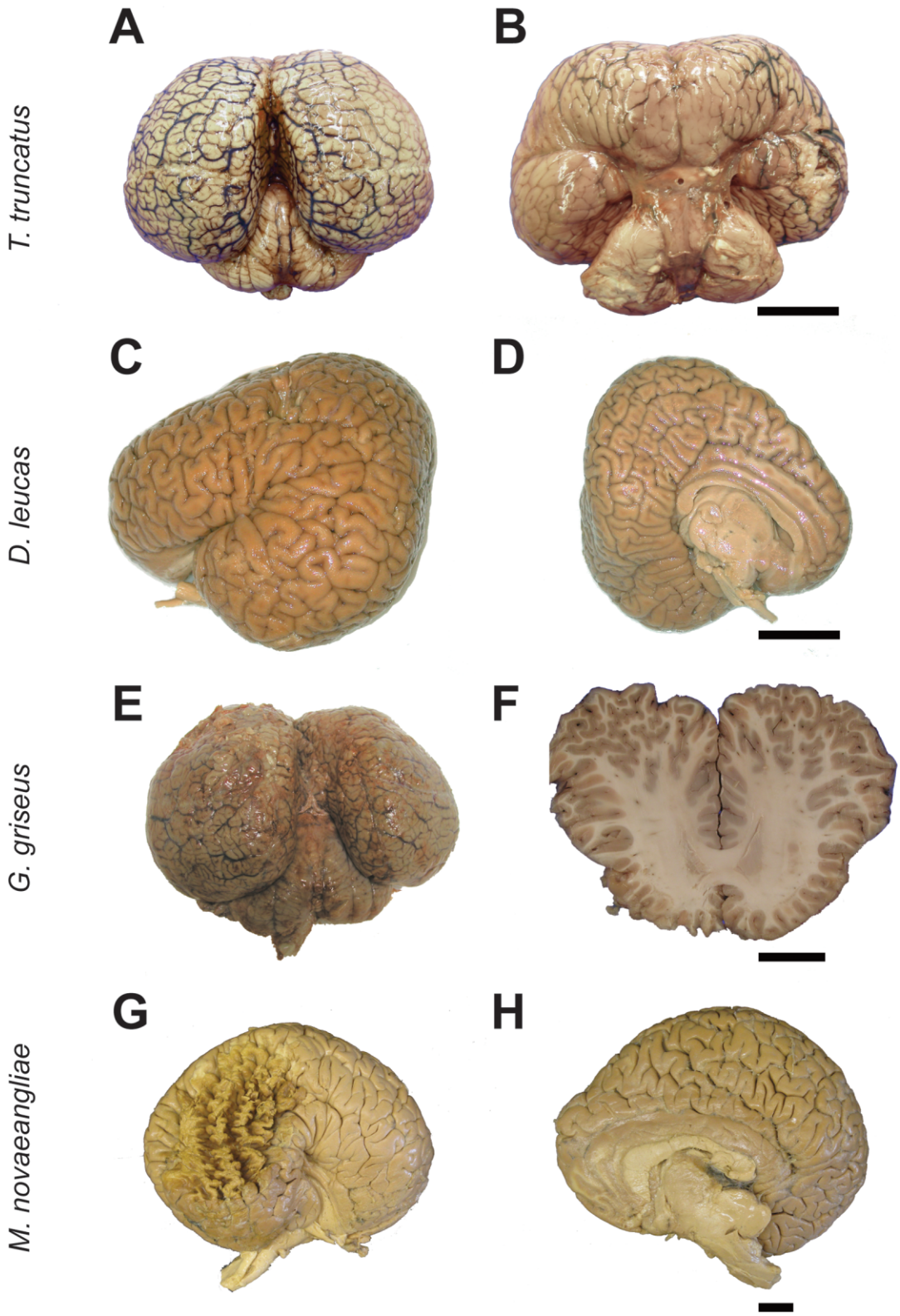

Figure 1.
Macroscopic views of the brains of the cetacean species analyzed in the present study. Dorsal (**A**) and ventral (**B**) views of the brain of a bottlenose dolphin; lateral (**C**) and midline (**D**) views of the left hemisphere of the brain of a beluga whale; dorsal view (**E**) and coronal slab at the level of the genu of the corpus callosum (**F**) of the brain of a Risso's dolphin; lateral (**G**) and midline view (**H**) of the right hemisphere of the brain of a humpback whale. Note the large size of the brains and the complex gyral pattern. The lateral aspect of the parietal lobe of the humpback whale brain sustained damage when the specimen was removed from the skull (G). This, however, did not affect the present study. The brains are not shown to scale. Scale bars = 3 cm.

TABLE 1. Average Values of Brain Weight, Body Weight, and EQ for the Analyzed Species[1]

Species	Brain weight (g)	Body weight (g)	EQ
T. truncatus	1,824	209,530	4.14
G. griseus	2,387	328,000	4.01
D. leucas	2,083	636,000	2.24
M. novaeangliae	6,411	39,295,000	0.44

[1]Brain weight and body weight were unavailable for most of the specimens in this study. These values were taken from Marino et al. (2004) and Hof et al. (2005).

A map of the sampled regions displaying the limits of the ROIs in an odontocete (*T. truncatus*) and a mysticete (*M. novaeangliae*) is shown in Figure 2. These boundaries were based on comprehensive descriptions of the anatomy of the bottlenose dolphin brain by Jacobs et al. (1971,1979, 1984), Morgane et al. (1980, 1982), Manger et al. (1998), and Hof et al. (2005) for the odontocetes and on the description of the structure of the cerebral cortex of the humpback whale brain by Hof and Van der Gucht (2007). Briefly, the cingulate cortex was identified as the cortical domain located ventrally to the splenial fissure and ventral to it on the midline of the hemisphere. Anterior and posterior cingulate cortices were identified on the basis of their cytoarchitecture as described by Morgane et al. (1982) and Hof and Van der Gucht (2007). The insular cortex was identified as the cortex distributed on the medial wall of the pocket formed by the Sylvian fissure, and the distinction between anterior and posterior insular cortices was based on cytoarchitectural criteria of Jacobs et al. (1984) and Hof and Van der Gucht (2007). The frontoinsular cortex was defined as the cortical domain that forms an extension from the anterior part of the insular cortex and merges with the posterior aspect of the orbital lobe (Hof and Van der Gucht, 2007). The frontopolar cortex was identified as the cortical domain that encompasses the polar gyri at the tip of the frontal lobe and ventrally the cortex that merges with the frontoinsular cortex (Hof and Van der Gucht, 2007). Some examples of the cytoarchitecture of these cortical domains are presented in Figure 3.

Stereologic design

For stereologic quantification, we selected every tenth section from the bottlenose dolphin, the Risso's dolphin, and the beluga whale and every twentieth section from the humpback whale, in view of the larger size of the humpback whale brain compared with the smaller odontocetes. Moreover, in the four examined species, VENs were found to be distributed beyond the FI into the whole anterior part of the insula (Hof and Van der Gucht, 2007). Thus, when referring to VENs distribution in the cetacean insula, we use the term "anterior insula" (AI) instead of "frontoinsular cortex" (FI).

All the quantitative analysis were performed on a stereology workstation equipped with a Zeiss Axiophot photomicroscope; Plan-Neofluar objectives ×2.5 (N.A. 0.075), ×40 (N.A. 0.75), ×40 LD (N.A. 0.6); Plan-Apochromat objectives ×10 (N.A. 0.32) and ×20 (N.A. 0.8; Zeiss, Thornwood, NY); a motorized stage (Ludl Electronics, Hawthorne, NY); an Optronics MicroFire digital camera (Optronics, Goleta, CA); and stereology software (StereoInvestigator; MBF Bioscience, Williston, VT). Starting with a random section number, a systematic sampling (every tenth or twentieth Nissl-stained sections depending on the specimen) throughout the ROIs was performed. The boundaries of the ROIs in each section were traced at low magnification (×2.5) on the computer display. The whole cortical thickness was included in the traced area. Within the cortical ROIs, additional subregions, including exclusively layers III and V, were traced separately.

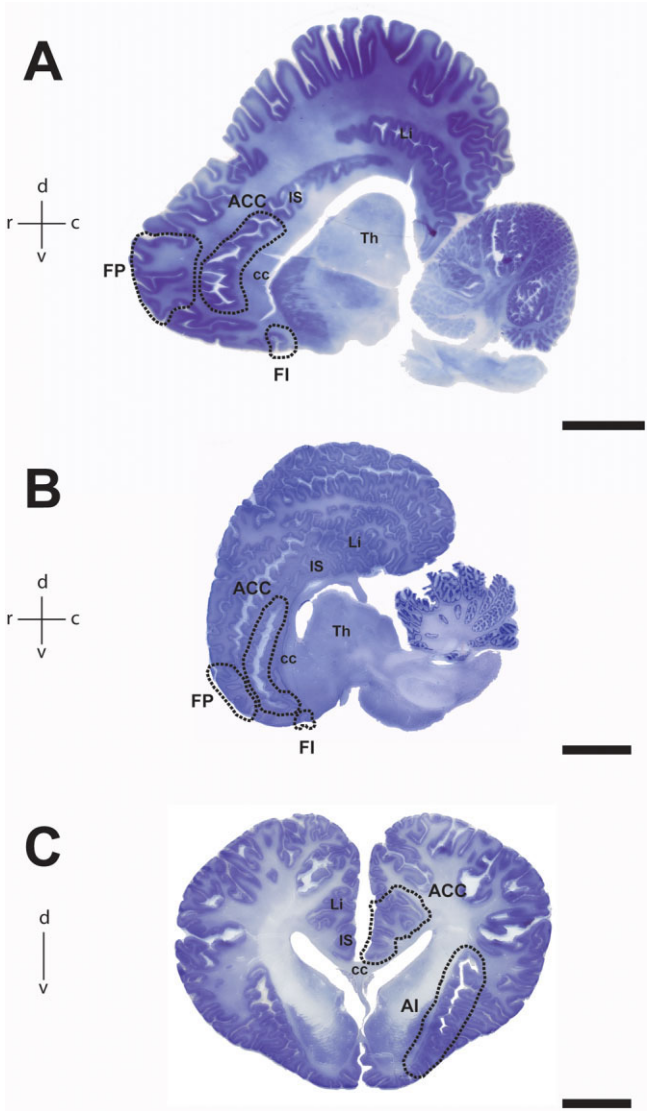

Figure 2.
Nissl-stained parasagittal (**A,B**) and coronal (**C**) sections of the brain of the right hemisphere of a humpback whale (A) and of a bottlenose dolphin (B,C) showing the cortical regions of interest: anterior cingulate cortex (ACC), frontoinsular cortex (FI), anterior insular cortex (AI), and frontopolar cortex (FP). The location of the regions of interest in the brain of the humpback whale and of the bottlenose dolphin are shown as representative of the mysticete and odontocete brains, respectively; they occur within the same landmarks in either suborder. CC, corpus callosum; IS, intercalate sulcus; Li, limbic fissure; Th, thalamus. Scale bars = 2.5 cm.

Total VEN numbers were estimated, within each subregion's contour, by using the optical fractionator (West et al., 1991). However, the relatively small number of VENs and their peculiar distribution in clusters required that, to ensure that every VEN would have an equal probability of being counted,

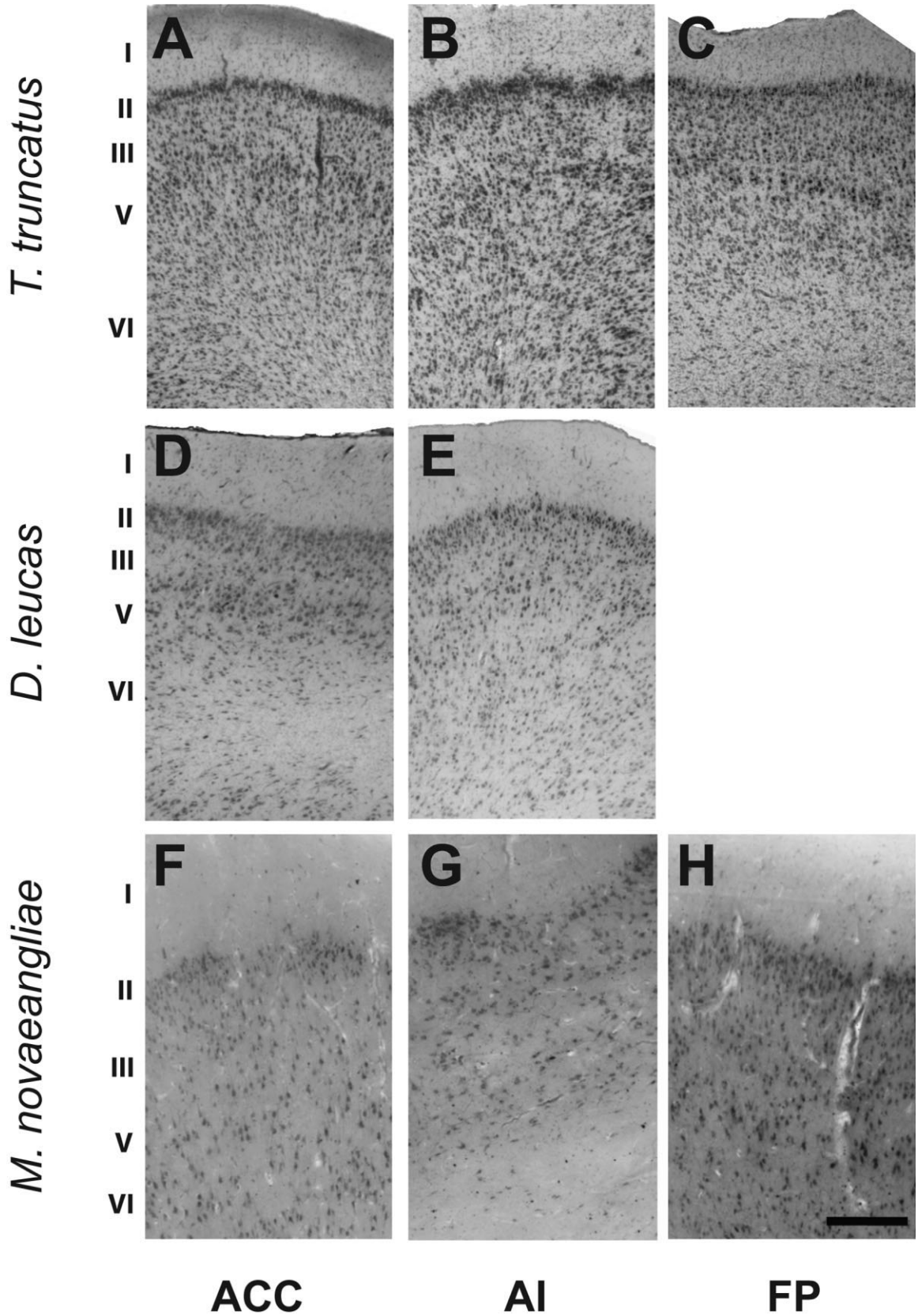

Figure 3.
Comparative structure of the anterior cingulate (**A,D,F**) and anterior insular (**B,E,G**) and frontopolar (**C,H**) cortices of the brain of a bottlenose dolphin (A–C), a beluga whale (D,E), and a humpback whale (F–H). Aside from the overall lower cellular density of the humpback whale cortex (F–H) compared with the smaller brain species (A–E), the cytoarchitecture of the ACC is comparable in all of the species. A high degree of clustering of layer II is present in the insular cortex of the humpback whale, but not to the same extent in the smaller odontocetes. ACC, anterior cingulate cortex; AI, anterior insula; FP, frontopolar cortex. Cortical layers are indicated by Roman numerals. Scale bar = 400 μm.

TABLE 2. Summary of Parameters Used for the Optical Fractionator in the Analysis of VEN Numbers[1]

Parameter	ROI	*T. truncatus*	*G. griseus*	*D. leucas*	*M. novaeangliae*
Number of sections	ACC	17	24	16	5
	AI			26	24
	FP				13
Number of microscopic fields	ACC	11,375	17,845	1,382	29,718
	AI			1,520	54,540
	FP				58,267
Mean section thickness after processing (μm)		30	30	14	14
Area of the unbiased counting frame (μm^2)		20,900	20,900	20,900	42,500
Disector height (μm)		28	28	12	12
Guard zones (μm)		1	1	1	1

[1]ACC, anterior cingulate cortex; AI, anterior insula; FP, frontopolar cortex; ROI, region of interest.

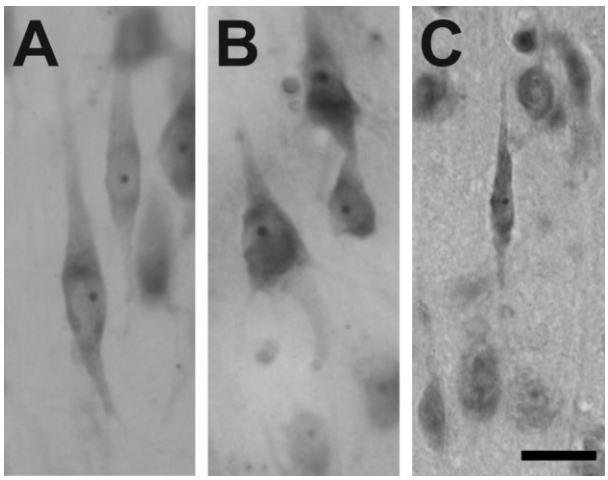

Figure 4.
Comparison of the typical morphology of VENs (**A**) with pyramidal neurons of layer V (**B**) and a fusiform cell of layer VI in the AI of the beluga whale (**C**). Note the large difference in size between VENs and the layer VI fusiform neuron. Scale bar = 40 μm.

we perform an exhaustive count. To achieve this, the dimension of the sampling grid was set equal to the dimension of the counting frame. To prevent bias from an uneven surface of the section or to the loss of nucleoli during the cutting procedure, guard zones at the top and at the bottom of the section were established. The size of the guard zones was set to allow the disector height to sample at least 80% of the tissue thickness as measured after processing. All stereologic parameters were set after taking into account the degree of shrinkage caused by histological processing (approximately 60% in our specimens; see below). Details on the stereologic parameters used for optical fractionator analyses of VEN number are summarized in Table 2.

The typical VEN morphology is shown in comparison with that of pyramidal and fusiform neurons in Figure 4. Neurons were identified as VENs in Nissl-stained sections if they were present either in deep layer III or in layer V of the ACC, AI, and FP and displayed the morphological features presented in Figure 5. The nucleolus was used as the counting reference, and VENs were counted when the nucleolus came into focus inside the counting frame within the disector height. Only the VENs that had their nucleolus totally or partially inside the counting frame and not crossing the exclusion lines of the frame were counted.

The total number of neurons of the available areas containing VENs was assessed in each species using the optical fractionator for estimation of the VEN fraction of the total neuronal population. The software defined a systematic-random-sampling sequence of frames within the outlines of the ROIs, in which neurons were quantified. Because of differences in the processing protocols and in the size of the ROIs between specimens, the parameters set for the total neuron quantification changed between animals, because every animal was considered separately. The dimensions of the sampling grid were set to sample at least 200–300 neurons per specimen, and the disector height was selected to sample at least 80% of the section thickness. Guard zones of 1 μm were used on the top and the bottom of every section. Details on the stereologic parameters used for the optical fractionator in estimating total neuron numbers are summarized in Table 3. Neurons (including pyramidal cells and interneurons) were counted with the same inclusion criteria as described above for VENs if they had pale nuclei, dark and recognizable nucleoli, and a relatively large soma.

Changes in tissue volume resulting from histological processing are a potential source of bias for estimates of the cell volume that depend on the fixation and embedding protocol used (Schmitz and Hof, 2005). When studying cetacean brains, the use of standardized protocols is difficult owing to the nature and rarity of the specimens. In fact, several brain specimens came from histological collections established decades ago, others from captive animals, and others from stranding events, making it nearly impossible to obtain brains processed under identical conditions. In the present study, we attended to such potential sources of bias as follows. The shrinkage in the z-direction was compensated for all the specimens examined by measuring systematically the thickness of the sections at selected intervals. Although we could minimize the shrinkage in the x-y direction in the brain of one of the humpback whales, the bottlenose dolphin, and the Risso's dolphin by ensuring that the sections were mounted soon after cutting and before staining (Schmitz et al., 2002), we had no control on the processing of the brain tissue of the beluga whale or the second humpback whale, which were embedded in celloidin, an embedding medium that considerably increases the shrinkage of the tissue. However, Schmitz et al. (2000) showed that the total number of pyramidal cells obtained in methacrylate-embedded sections vs. cryostat sections in the mouse hippocampus were comparable. It should also be noted that the optical fractionator does not rely on the calculation of an estimate of an actual volume of reference, and as such our number estimates are not affected by differential shrinkage.

The volume of every counted VEN was assessed by using the optical rotator (Tandrup and Jensen, 1997), a stereologic

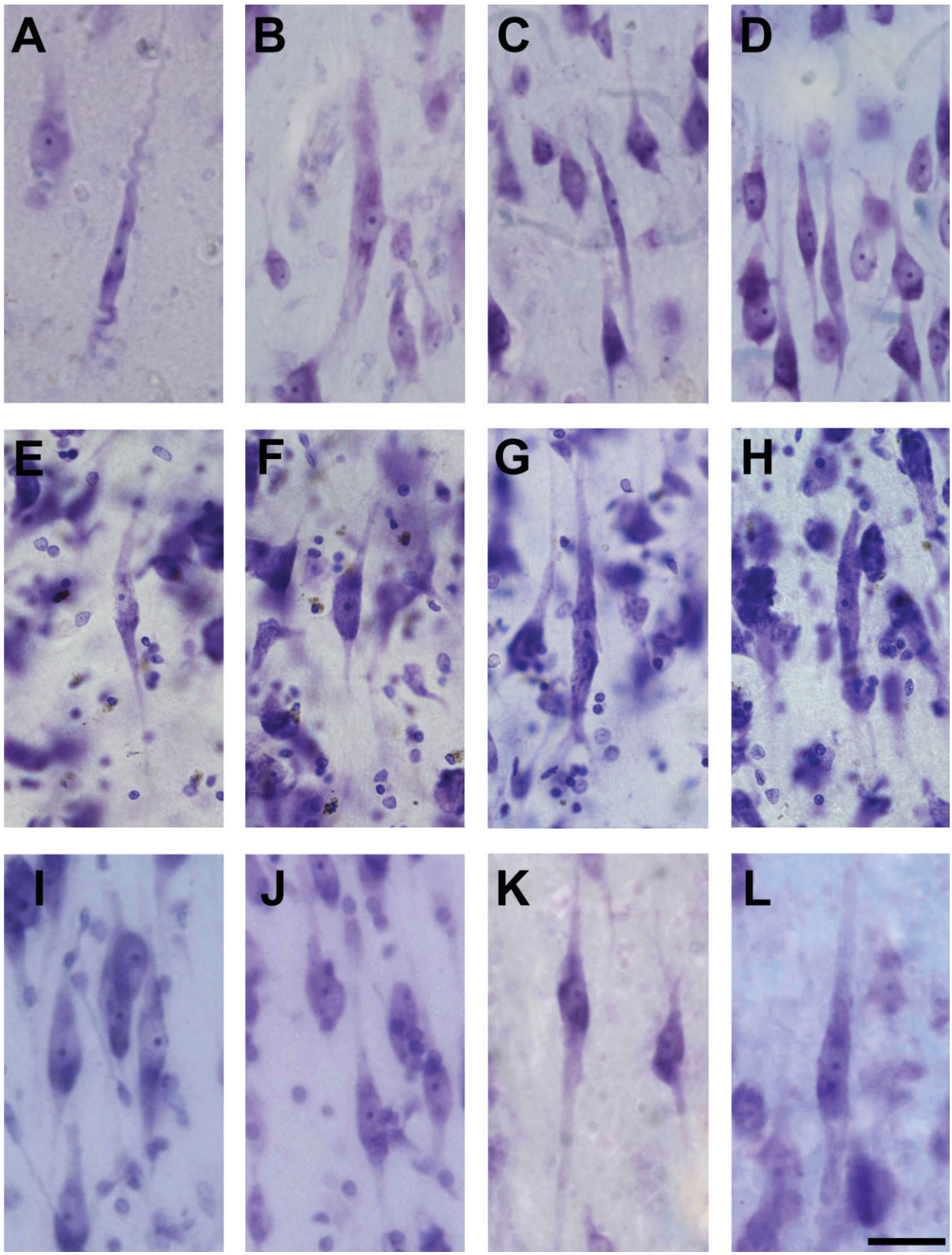

Figure 5.
Morphology of VENs. Anterior cingulate cortex (**A,B**) and anterior insular cortex (**C–E**) of the beluga whale, anterior cingulate cortex of the Risso's dolphin (**F–H**), anterior cingulate cortex of the bottlenose dolphin (**I,J**), and frontopolar cortex of the humpback whale (**K,L**). Scale bar = 40 μm.

TABLE 3. Summary of Parameters Used for the Optical Fractionator in the Analysis of Total Neuron Numbers[1]

Parameter	ROI	*T. truncatus*	*G. griseus*	*D. leucas*	*M. novaeangliae*
Number of sections	ACC	7	12	16	
	AI			26	26
Number of microscopic fields	ACC	183	500	478	
	AI			499	226
Area of the unbiased counting frame (μm^2)		3,600	3,600	3,600	3,600
Sampling grid size (μm)		2,000 × 2,000	2,000 × 2,000	1,000 × 1,400	5,000 × 5,000

[1]ACC, anterior cingulate cortex; AI, anterior insula; ROI, region of interest.

TABLE 4. Summary of Parameters Used for the Optical Rotator Analysis of Each Neuronal Type

Parameter	VENs	Pyramidal cells	Fusiform cells
Focal plane separation (μm)	2	3	2
Grid line separation (μm)	9	6	6
Optical slab thickness (μm)	7	7	4
Number of grid lines	4	4	4
Slab type	Isotropic	Isotropic	Isotropic

three-dimensional local estimator of volume that samples focal planes through the central region of a cell, thereby avoiding problems with the identification of its top and bottom borders. For limitations resulting from the nature of the preparations, the volume of VENs in one of the humpback whale could not be measured with a sufficient degree of precision with the optical rotator. The brain sections of this specimen were coverslipped with thick coverglass and did not allowed a sharp image of each focal plane throughout the thickness of the section as required by the optical rotator. Assuming that intraspecific differences in the volume of VENs would not to be found, we investigated sections from only one humpback whale to assess the average volume of VENs in this species. The thin coverslips used on the histological sections of the brain of this specimen allowed the measurement of the VEN volume with the optical rotator. Details on the stereologic parameters used for the optical rotator are summarized in Table 4.

Moreover, because the major histological collections of human, apes, and cetacean tissue are embedded in celloidin and coverslipped with thick coverglasses, we considered it important to define the degree of over- or underestimation of the VEN volume caused by a probe that can be used in such materials, such as the nucleator (Gundersen, 1988). The nucleator is a two-dimensional local probe that measures the cross-sectional area of a particle in only one focal plane and assumes uniformity in all directions. However, VENs are not isotropic, and any estimate obtained with the nucleator will inevitably be inaccurate. We investigated sections from the celloidin-embedded humpback whale brain with a six-rays nucleator and compared the VEN volume estimates with the values obtained for the other humpback whale with the optical rotator. Again, we assumed that there are no differences in VEN volume within the same species. The average VEN body volume assessed with the optical rotator was 6,188 ± 948 μm^3, and the average value assessed with the nucleator in the other specimen was 5,870 ± 1,311 μm^3, yielding an overall underestimation of about 5% with the nucleator in these celloidin-embedded sections. However, this difference also reflects the possible degree of shrinkage that different histological protocols (in this case, dehydration and celloidin-embedding vs. freezing of formalin-postfixed materials) may cause. The difference in cell volume estimates being rather small, based on our results, the use of one probe or the other should not significantly bias the average measured volume. However, to address the potential bias when comparing volume estimates obtained in specimens prepared with different histological protocols, we decided to express the VEN volume as a "VEN volume index" given by the ratio of the average VEN volume to the average pyramidal cell volume in each specimen. In this way, our volume estimates provide values unaffected by shrinkage artifacts. By using the same stereologic procedures, we estimated the individual volumes of a smaller sample of pyramidal neurons in layer V and of smaller fusiform neurons in layer VI (approximately 100 for each cell type in every specimen, for comparison with VEN volumes). Details on the stereologic parameters used for the optical rotator in each cell type are summarized in Table 4. Quantitative and volumetric estimates of VENs and pyramidal and fusiform neurons were made with the ×40 (N.A. 0.75) or the ×40 LD (N.A. 0.6) objectives, depending on the quality of the histological preparations. VEN densities were not calculated given their uneven and clustered distribution in all regions, which prevents the elaboration of meaningful and reliable density estimates.

Photomicrographs were edited for brightness and contrast in Adobe Photoshop. Maps of VEN distribution were imported and graphically adjusted in Adobe Illustrator.

Statistical analysis

Total VEN numbers were obtained in only one specimen per species, so statistical analysis was not possible to perform. The Levene test was used to define whether the variances were homogeneous within the volumetric measurements. Because the volume of every counted VEN was measured but volumetric data of the pyramidal and fusiform cells was based on a sample of 100 neurons, we had to normalize group sizes. To achieve this, the interquartile range was calculated within every neuron type data set, and the measurements falling outside this range were excluded from the analysis. For the sets of data falling between the first quartile (Q1) and the third quartile (Q3), we randomly chose a sample of 50 measurements (lists were randomized by random.org, and the first 50 values from the lists were chosen) that was used for further analysis. We used the nonparametric Kruskal-Wallis ANOVA and Dunn's post hoc tests to determine whether there were significant differences in volume among VENs and pyramidal and fusiform neurons among and within species. To investigate possible correlation between the VEN volume, brain weight, body weight, and EQ, we used the nonparametric Spearman's correlation test. EQ data were obtained from Marino (1998), Marino et al. (2004), and Hof et al. (2005). EQ were calculated using the formula EQ = brain weight/0.12 (body weight)$^{0.67}$ (Jerison, 1973).

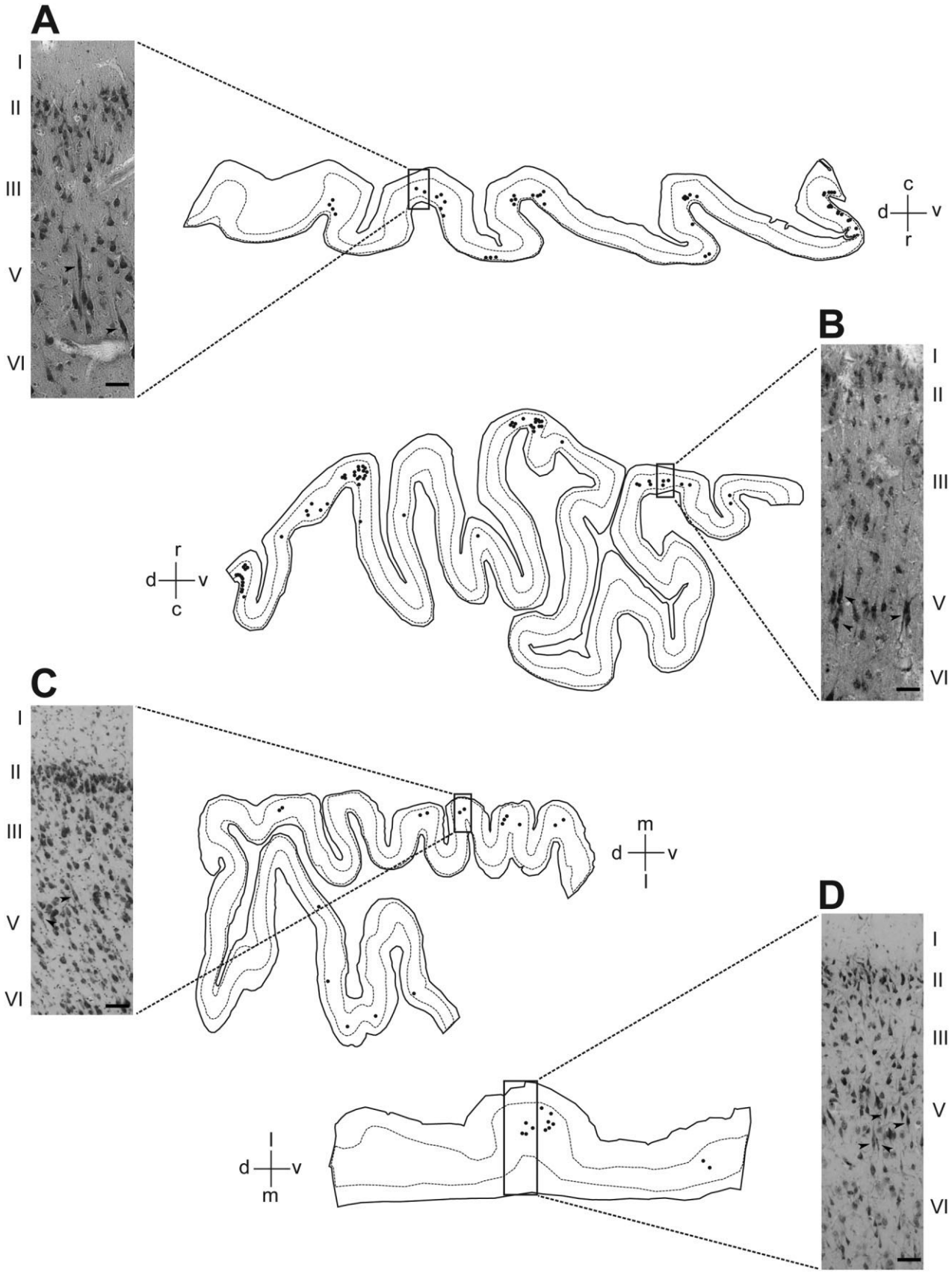

Figure 6.
Maps of the neocortical distribution of VENs. Anterior insular cortex (**A**) and frontopolar cortex (**B**) of the humpback whale, anterior cingulate cortex of the bottlenose dolphin (**C**), and anterior insular cortex of the beluga whale (**D**). The ROI (whole cortex) is outlined by a solid line, and layers III and V are outlined by a dashed line. Every dot corresponds to one VEN (see corresponding arrowheads on the microphotographs). VENs are located in deep layer III and layer V, clustered at the crown of the gyri, and only scattered cells are present along the banks of the sulci. Cortical layers are indicated by Roman numerals. Scale bars = 100 μm.

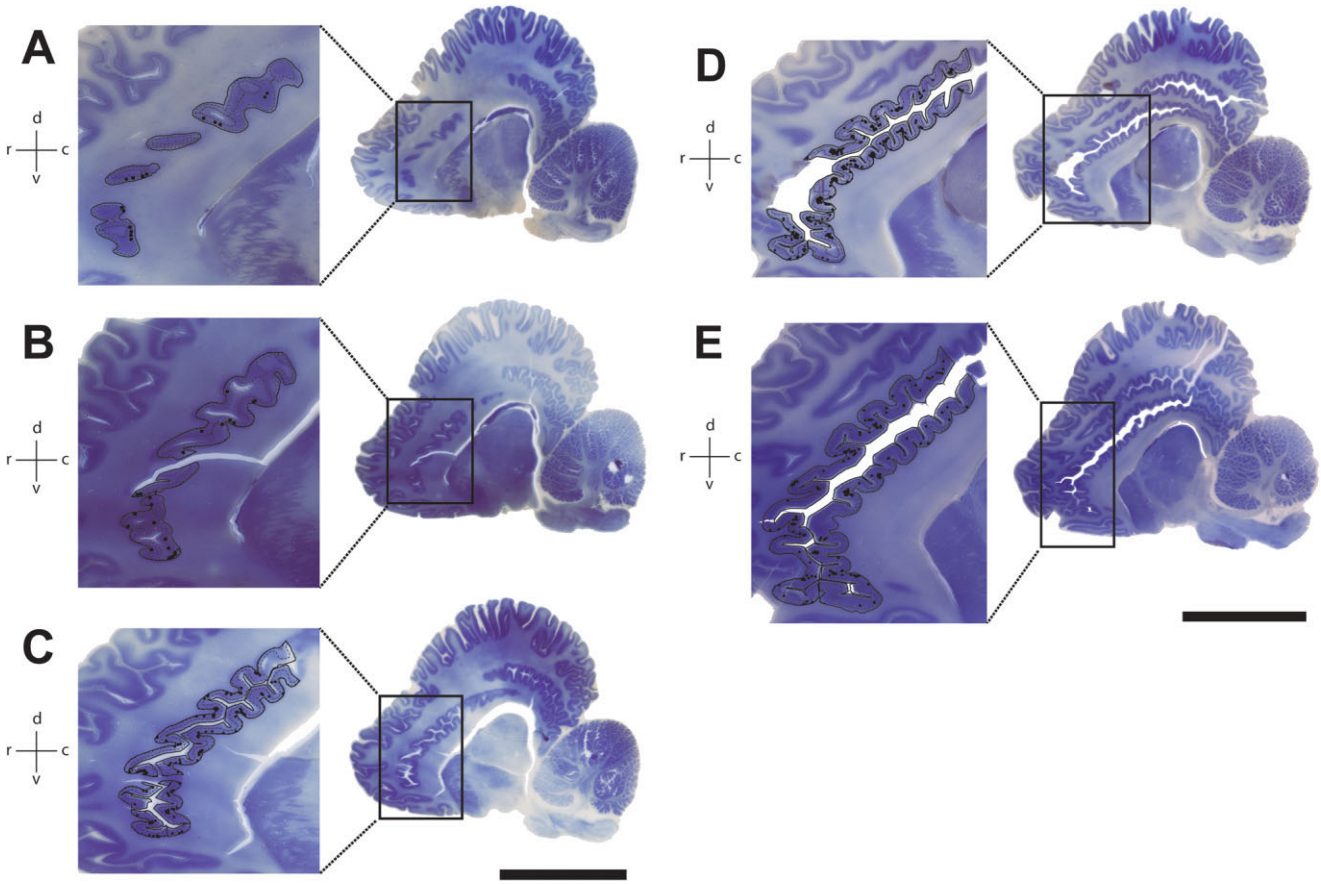

Figure 7.
A–E: Maps showing the landmarks of the anterior cingulate cortex (ACC) and the pattern of distribution of VENs in the humpback whale. The ROI (whole cortex) is outlined by a solid line, and layers III and V are outlined by a dashed line. Every dot corresponds to one VEN. VENs are clustered at the crown of the gyri, and fewer are present along the banks of the sulci. Scale bars = 6 cm (for the whole brain).

RESULTS

VENs were observed in all of the examined species and regions. Their morphology was easily distinguishable, and they were present in layer V and deep layer III (Fig. 6). As previously reported for the humpback whale (Hof and Van der Gucht, 2007), VENs predominantly assemble in small clusters, generally of three to five cells, near the crown of the gyri in the ACC, AI, and FP, whereas more scattered VENs are observed along sulcal banks (Figs. 6–9). Most of the VENs had a stout cell body with straight and long apical and basal dendrites departing from the soma (Fig. 5D–F,I–L). However, a few VENs were extremely slender, with very long apical and basal dendrites almost as thick as the cell body (Fig. 5B,C,H). Others had an elongate cell body with thin and curly basal and apical dendrites (Fig. 5A). Occasionally, we observed cells with the basal dendrite divided into two branches (Fig. 5G). These morphologies were observed in all of the investigated species and cortical regions.

The number of VENs in the regions of interest was expressed as a percentage of VENs from the estimated total number of neurons in that region and species (Table 5). Unfortunately, because of the availability of the materials, not all of the ROIs could be investigated in every species, and the comparisons of VEN quantitative data are based only on the available regions. Also, it should be noted that the number of sampled neurons, and thus the estimated total numbers, do not represent exhaustive counts for the entire ROIs considered, except in the case of *M. novaeangliae*.

A comparison of VEN numbers among species was possible only on the basis of our findings in the ACC, the only region available for all the four species examined. Within the ACC, the higher number of VENs was observed in the humpback whale, whereas the quantitative data for bottlenose dolphin, Risso's dolphin, and beluga whale were fairly comparable (Fig. 10B). Comparisons among ROIs were possible only for the humpback whale, for which all the three regions were available (Table 5). The numbers of VENs in the ROIs were in this case comparable among the three regions (Fig. 10C). Overall, the percentage of VENs from the estimated total neuron numbers was consistently low across species and varied from 0.01% to 0.06%, depending on the region. Interestingly, among all of the regions and species, the insular cortex of the beluga whale showed the highest percentage of VENs from the total neuronal population estimated for the species in this specific ROI (Table 5). However, the observed higher percentage of VENs is due not to a major increase in

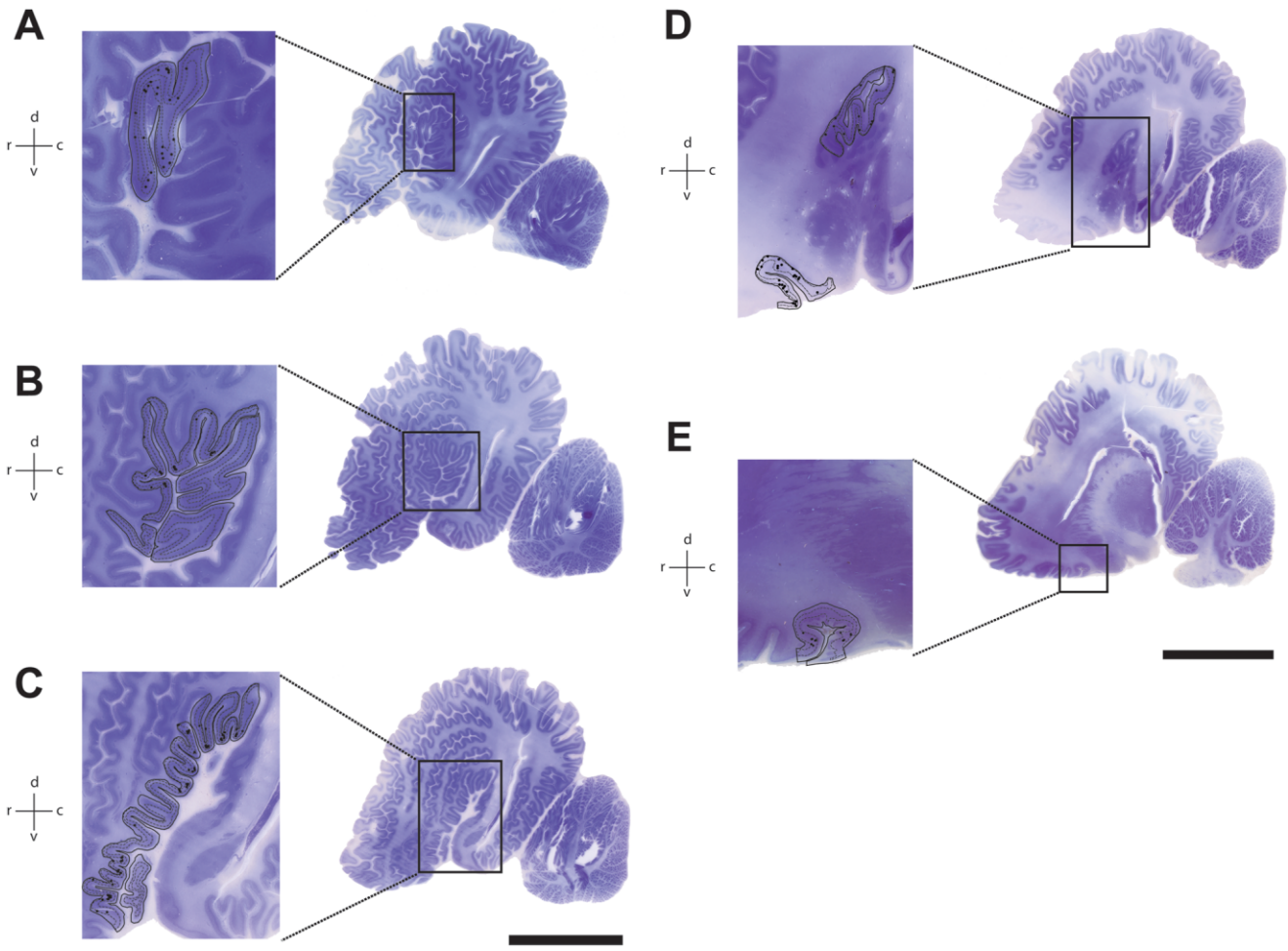

Figure 8.
A–E: Maps showing the landmarks of the anterior insula (AI) and the pattern of distribution of VENs in the humpback whale. The ROI (whole cortex) is outlined by a solid line, and layers III and V are outlined by a dashed line. Every dot corresponds to one VEN. Scale bars = 6 cm.

total VEN number in this species but rather to a lower total number of neurons.

Volumetric estimates show that, similarly to the case in humans and great apes (Nimchinsky et al., 1999), the volume of VENs in cetaceans is larger than that of layer V pyramidal neurons and considerably larger than layer VI fusiform neurons (Table 6). Specifically, within our specimens, VENs were found to be 8–43% larger than pyramidal neurons of layer V and 54–73% larger than fusiform neurons of layer VI, depending on the species. Volume estimates, expressed as "VEN index" (ratio between the average volume of VEN and the average volume of pyramidal neurons for each species), indicate that, within the studied species, the largest index was found in the humpback whale, followed by the bottlenose dolphin, the beluga whale, and the Risso's dolphin with very close indices (Fig. 10A). Because the average variation in pyramidal cell somatic size among species is only 14%, we consider the variation in indices to reflect differences in the volume of VENs. In this view, as expected, our results show that the larger VENs belong to the humpback whale, whereas the volume estimates of VENs of the three odontocete species are fairly comparable. The somatic volume of VENs was found to be significantly different among species for all comparisons ($P < 0.001$), except for the Risso's dolphin and the beluga whale. Moreover, all differences in volume among neuron types within any of the species were found to be significant ($P < 0.001$), except for between VENs and pyramidal cell volumes in the Risso's dolphin, which had smaller VENs compared with other species (Table 6, Fig. 10A). In contrast to what has been reported for great apes (Nimchinsky et al., 1999), the raw VEN volumes did not, in our sample, show any significant correlation with the brain weight, body weight, or EQ (see Table 1; Spearman's rank order correlation: r = 0.20, $P = 0.91$; r = 0.40, $P = 0.75$; r = −0.40, $P = 0.75$, respectively).

DISCUSSION

Considering the highly divergent evolutionary history of cetaceans and primates (Kumar and Hedges, 1998), cetaceans evolved independently a very large and convoluted brain, an extremely expanded neocortex, and very high EQs. Although several hypotheses have been formulated to explain the reasons of such an increase in size and complexity, it is now widely accepted that the enlargement of the cetacean

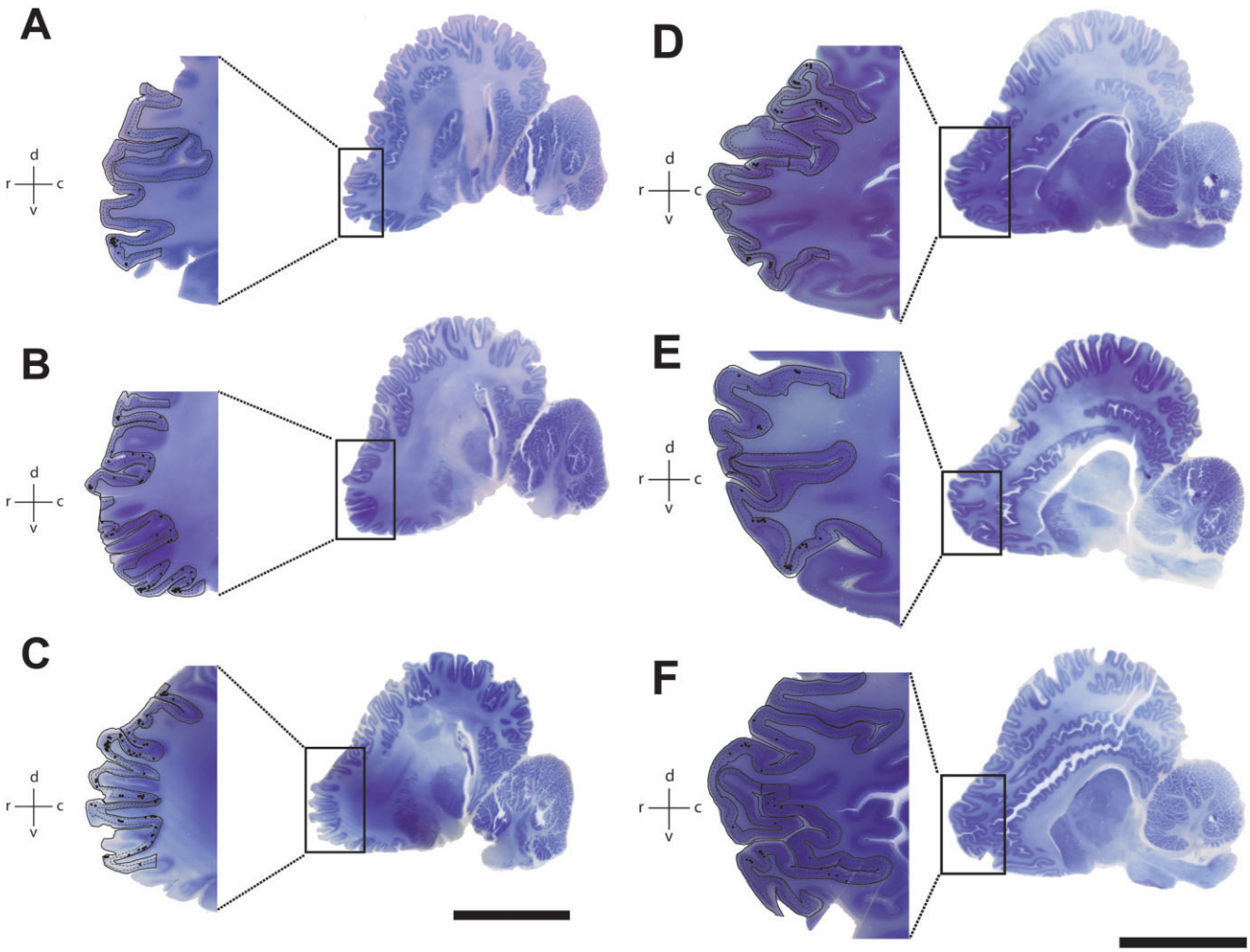

Figure 9.
A–F: Maps showing the landmarks of the anterior frontopolar cortex (FP) and the pattern of distribution of VENs in the humpback whale. The ROI (whole cortex) is outlined by a solid line, and layers III and V are outlined by a dashed line. Every dot corresponds to one VEN. Scale bars = 6 cm.

brain was driven by evolutionary selective pressures acting on complex cognitive abilities (for review see Marino, 2007). Anatomical evidence such as the enlargement and the histological complexity of the frontopolar region (Hof and Sherwood, 2005; Hof and Van der Gucht, 2007) and of the anterior cingulate and insular cortices (Jacobs et al., 1979; Hof and Van der Gucht, 2007) support this view. These regions are known to be involved in judgment, attention, intuition, and social awareness in primates (Allman et al., 2005).

The occurrence of VENs in all of the cetacean species we analyzed is striking. The predominant distribution of VENs in clusters and the regional distribution pattern comparable to that seen in humans and great apes makes their presence in the cetacean brain a particularly interesting neuroanatomical feature from an evolutionary perspective. In light of the phylogenetic distance between hominids and cetaceans and the absence of VENs in the other species analyzed so far, VENs can be considered to be the product of a process of convergent evolution rather than the product of postnatal mechanical factors that would have affected the morphology and distribution of relatively few neurons in restricted cortical domains, particularly in locations subject to bending stresses such as the crown of gyri. In fact, in his original paper, Von Economo (1926) described the process of "spindling" of the cortical elements as a process he considered common to all cell types in the neocortex and that he saw as responsible for the enhancement of the sharp contrast in morphology between "VENs" and surrounding pyramidal cells.

Taken together with our findings of the presence of VENs in three small odontocetes, the recent discovery of VENs in both the African elephant (*Loxodonta africana*) and the Indian elephant (*Elephas maximus*; Hakeem et al., 2009) provides support to the concept that VENs represent a possible obligatory neuronal adaptation in very large brains, permitting fast information processing and transfer along highly specific projections and that evolved in relation to emerging social behaviors in select groups of mammals. Cetaceans form complex societies in which individuals relate to each other depending on

TABLE 5. Results of Stereologic Estimates of Total VEN Numbers in the Investigated Species and Cortical Regions[1]

Species	ROI	Estimated VENs RH	Estimated VENs LH	VENs (%)	CE
T. truncatus	ACC		1,850		0.07
	SUBG		600	0.009	0.13
G. griseus	ACC	1,430			0.08
	SUBG	580		0.004	0.13
D. leucas	ACC	370		0.012	0.16
	AI	1,910		0.061	0.07
M. novaeangliae	ACC	24,180			0.04
	AI	28,770		0.027	0.03
	FP	24,900			0.03

[1]VEN numbers in the odontocetes represent only the available blocks from the ROI and are therefore underestimates. Moreover, the estimates were obtained in the only available hemisphere in each specimen. The right hemisphere of *T. truncatus* and the left hemispheres of *G. griseus*, *D. leucas*, and *M. novaeangliae* as well as the FP in the odontocetes were not available, because they had been used previously or were distributed to other investigators. ACC, anterior cingulate cortex; AI, anterior insula; FP, frontopolar cortex; SUBG, subgenual cortex; LH, Left hemisphere; RH, Right hemisphere; ROI, region of interest; VENs (%), percentage of VENs calculated from the total number of neurons in the cortical area of interest; CE, Coefficient of error (calculated as the inverse of the square root of the number of cells counted). The CE measures the accuracy of the estimates and takes into account the distribution of the counted particles in the tissue and the total number of particles sampled (Schmitz and Hof, 2005). Because of the uneven and clustered distribution of VENs and their low numbers, CE values are sometimes higher than desirable (>0.1) and are not optimal indicators of the accuracy of the estimates, which in these cases resulted from exhaustive enumerations.

their hierarchical position; they have been reported to create nested alliances, to use tools, to be able to learn symbolic artificial languages, and, as with elephants, to show self-awareness as demonstrated by tests of mirror self-recognition (Herman et al., 1984, 1993; Krushinskaya, 1986; Connor et al., 1992; Reiss and Marino, 2001; Krutzen et al., 2005; Plotnik et al., 2006; Lusseau, 2007; Marino et al., 2007, 2008; Poole and Moss, 2008).

The typical long and wide axons of VENs have been proposed to play a key role in the organization of the connectivity in cognition-related networks in large brains (Allman et al., 2002, 2005). In this context, it is very interesting to stress the presence of VENs in the frontopolar region in these cetaceans. In fact, there has been a long debate regarding whether there might be a cortical region corresponding to the prefrontal cortex of primates in cetaceans. The cetacean frontopolar cortex is extremely expanded and shows a very distinct cytoarchitecture compared with its adjacent fields. The presence of VENs in this cortical domain suggests that this area is, as in hominids, endowed with high-level cognitive functions and that the possible cortical homolog of the prefrontal cortex is very well developed and specialized in cetaceans. It is indeed interesting to note that VENs have recently been reported in the dorsolateral prefrontal cortex in humans (Fajardo et al., 2008), reinforcing the notion that these cortical domains may indeed represent functional homologs in hominids and cetaceans.

The presence of VENs in the ACC, AI, and FP of the cetacean brain is not a direct demonstration of high-level cognition, but it is consistent with the existence in these species of complex cognitive abilities and hints at a neuronal specialization that may underlie their expression. It is interesting, in this light, to point out that cetaceans and primates possess the highest levels of encephalization among vertebrates, with EQ values of 7.0 for modern humans, of between 1.5 and 3.0 for great apes, and of 4.5 for some odontocetes species, placing cetaceans second to humans, with EQs considerably higher than any other mammal (Marino, 1998; Marino et al., 2004). In great apes, the somatic volume of VENs was shown to be highly correlated with brain volume residuals (Nimchinsky et al., 1999). The present data show that VEN volume is not correlated with brain weight, body weight, or EQ. This lack of correlation may reflect not only the small sample size of the four species, three of which are very close in terms of brain size, to which our study was limited but also the fact that mysticetes are not particularly encephalized owing to their large body size (Marino et al., 2004). If a correlation of VEN volume with any of these parameters were to be observed, it would be more likely among the smaller odontocetes, assuming that VENs occur in all or most of these species. Moreover, the fact that, in the humpback whale, VENs, but not pyramidal or fusiform cells, are considerably larger than the same cell types in the examined odontocetes supports the possibility that a relationship between body size and VENs size exists. The present study was limited in this respect to three delphinoid taxa, and a more extensive sample of cetacean species to allow for a more complete representation of brain size variability, especially among the smaller bodied odontocetes, will be necessary to determine whether VEN volume is correlated with any of these parameters.

VENs are 42–79% larger than pyramidal neurons of layer V and 75–92% larger than fusiform cells of layer VI in great apes, depending on the species (Nimchinsky et al., 1999). The present results show that, even if the difference in somatic volume among neuronal types is statistically significant within a given species, the magnitude of this difference is less pronounced in cetaceans than in primates. Neuron size (and thus axon length and width) increases as a consequence of brain size increase. There is in fact evidence showing that, in large brains, the need to reduce metabolic firing costs and transmissions delays is prioritized over limiting an increase in neuronal size (Wang et al., 2008). However, there may be rules acting on the optimization of the conduction that constrain the maximum size and length that axons can achieve, thus inevitably influencing the somatic size of a particular neuron. It could be that, in the case of cetaceans, the increase in brain size could not be followed by the expected increase in VEN volume in order to keep the optimal efficiency of VEN conduction, thus explaining the less pronounced difference in somatic volume among neuronal types observed in these species compared with hominids.

In view of the fact that, for the three odontocetes, the blocks we analyzed included only a portion of the ROI, and therefore doubtless represent underestimates, whereas for the humpback whale we had access to the entire structure, we can use the latter to make comparison of absolute numbers of VENs between cetaceans and data available for humans, great apes, and elephants. Our results show that the absolute number of VENs in the humpback whale, at least in the AI, is fairly comparable to that in other species in which the FI was analyzed (for data on hominids and elephants VENs see Kaufman et al., 2008; Hakeem et al., 2009; Allman et al., 2009). In fact, there are overall twice as many VENs in the humpback whale FI/AI as in the Western lowland gorilla and elephant, numbers comparable to those in newborn humans and chimpanzees, but numbers 2.5 times lower than in human adults (Kaufman et al., 2008; Hakeem et al., 2009; Allman et al., 2009). It should, however, be kept in mind that VENs are present not only in the FI but also in the AI in the humpback whale, in

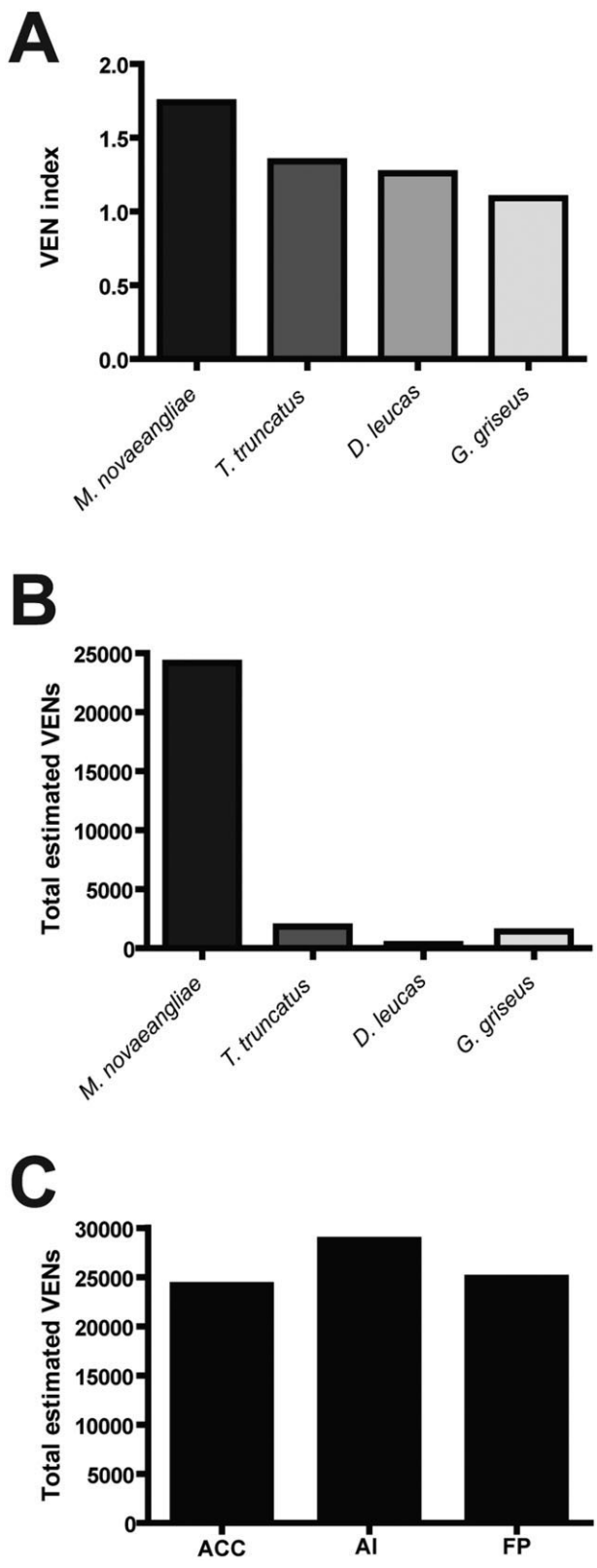

Figure 10.
Ratio of the average VEN volume to the average pyramidal cell volume "VEN index" (**A**) and total estimated numbers of VENs in the ACC of the four examined species (**B**) and in the three regions of interest of the humpback whale (**C**).

TABLE 6. Volume of Layer V VENs and Pyramidal Cell and Fusiform Cells of Layer VI[1]

Species	VENs	Pyramidal neurons	Fusiform neurons	VEN index
T. truncatus	4,449 ± 524	3,323 ± 310	1,436 ± 175	1.34
G. griseus	3,186 ± 479	2,923 ± 298	1,460 ± 158	1.09
D. leucas	3,406 ± 468	2,710 ± 347	1,248 ± 150	1.26
M. novaeangliae	6,189 ± 948	3,558 ± 393	1,662 ± 231	1.74

[1]Volumes are expressed as mean (μm^3) ± SD. The VEN index is the ratio between the average volume of VEN and the average volume of pyramidal neurons.

contrast to hominids and elephants in which they are mostly concentrated within FI, revealing a notable variant in the distribution of VENs among these three mammalian groups. The low percentage of VENs in the humpback whale compared with hominids and elephants thus is due mainly to the much higher number of total neurons and much larger AI in the whale. It should be added that very few quantitative data on the cetacean cortex are available (see, e.g., Tower, 1954; Kraus and Pilleri, 1969; Garey and Leuba, 1986; Schwerdtfeger et al., 1984; Haug, 1987; Poth et al., 2005; Eriksen and Pakkenberg, 2007), allowing for only limited comparison among studies resulting from differences in methods and investigated species. However, our estimates in a given cortical region, such as FI/AI, would generally not be inconsistent with previously published estimates of cortical neuron numbers.

With regard to odontocetes, and even considering that we could not exhaustively sample the relevant regions in these three species, the total number of VENs in this group is significantly lower than in hominids, elephants, and humpback whale (in spite of the high EQ of these small odontocetes). This may reflect the fact that, although VENs appeared early in the evolutionary history of modern whales, being present both in mysticetes and in the oldest family of toothed whales, the physeterids (Fordyce and Barnes, 1994), their distribution and numbers continued to evolve in the recent history of cetaceans, perhaps representing a certain degree of refinement in the projections that they may subserve. In this context, it will be interesting to investigate VENs in the brains of small physeterids such as the pygmy sperm whale (*Kogia breviceps*), and a small balaenopterid such as the minke whale (*Balaenoptera acutorostrata*), which incidentally possesses VENs in a distribution seemingly comparable to that in *M. novaeangliae* (Butti and Hof, unpublished observations). Moreover, the uneven distribution and overall low numbers of VENs (varying from under 1% to about 3% of the total number of neurons depending on the species and region) in the brain of all of the species in which they have been described thus far recall the distribution and density of other highly specialized neuronal populations such as the Betz and Meynert cells that are found only in layer Vb of the primary motor and in layer VI of the primary visual cortex, respectively, in primates (Hof et al., 2000; Rivara et al., 2003) and exhibit species-dependent morphologic and functional specialization (Sherwood et al., 2003). Even though the total numbers of VENs in the species in which they have been observed are rather variable, the presence of this peculiar cell type within the same regional and laminar pattern across divergent species indicates that the projections that VENs may provide are perhaps as specific as those furnished by neurons such as Betz and Meynert cells. What

their specific function might be, however, remains to be elucidated.

VENs send an axon out of the cerebral cortex, based on observations in post-mortem human brain after DiI labeling (Nimchinsky et al., 1995), but there is no direct evidence on their functional role owing to the fact that the species in which they occur make it impossible to use invasive approaches. The ACC and FI (and more generally the AI) are connected to the prefrontal and orbitofrontal cortices in macaque monkeys (Cavada et al., 2000; Ongür and Price, 2000; Barbas et al., 2003; Höistad and Barbas, 2008). The evidence that VENs send axons in the subcortical white matter in humans (Nimchinsky et al., 1995; Allman et al., 2005; Watson et al., 2006) and their selective presence in these reciprocally linked region of the cortex suggest that they may connect ACC and FI/AI (Craig, 2009). Also, as shown by human fMRI studies, the regions containing VENs are involved in high-level cognitive processing, such as feelings of empathy (Singer et al., 2004), guilt (Shin et al., 2000), embarrassment (Berthoz et al., 2002), and pain (Craig et al., 1996; Rainville et al., 1997), as well as judgement, social knowledge, and consciousness of visceral feelings (Craig, 2003, 2004, 2009). In this context, neuropathologic investigations in brains from patients with frontotemporal dementia, a disorder that disrupts several aspects of social functioning and self-awareness, have revealed a 74% reduction in VEN number. In these cases, many of the remaining VENs displayed severe morphologic alterations and abnormal accumulation of pathologic proteins (Seeley et al., 2006, 2007). In addition, their localization in layer V is suggestive of projections to subcortical regions, such as the amygdala, hypothalamus, and periaqueductal gray, to which the ACC and FI/AI are known to project in primates (Nimchinsky et al., 1999; Barbas et al., 2003; Hof and Van der Gucht, 2007). Altogether, VENs may be involved in the integration of emotions, vocalization control, facial expression, or social conduct as well as regulation of autonomic visceral, olfactory, and gustatory functions.

In conclusion, the specific distribution of VENs in the ACC, AI, and prefrontal cortex (FP in the case of cetaceans) of all of the species for which VENs have been described to date suggests that, in large brains, these regions of the cortex (and their specific networks) were shaped by comparable selective pressures, of which the VENs may be the evolutionary outcome. In the specific case of cetaceans, the presence of VENs in select areas of the brain in both cetacean suborders may be the anatomical basis for the observed behavioral cognitive convergences that, despite a long phylogenetic divergence, are widely recognized to be shared by primates and cetaceans. Moreover, given their selective vulnerability, study of the evolution of VENs and of their functional role and connectivity is necessary to further our understanding of the evolution of neocortical circuits that, when disrupted in human-specific neuropsychiatric illnesses, are responsible for the impairment of social and cognitive skills.

ACKNOWLEDGMENTS

The authors thank Drs. P.J. Morgane and I.I. Glezer for donation of the humpback whale and beluga whale brain specimens and the collections of histological slides, the Mediterranean Marine Mammals Tissue Bank of the University of Padova and Dr. B. Cozzi for generously providing materials from the bottlenose and Risso's dolphins, and Dr. C. Schmitz for valuable advice on stereologic procedures. We thank Drs. A.D. Craig, D.L. Dickstein, and M. Höistad for helpful discussions and B. Wicinski and S. Harry for expert technical assistance.

LITERATURE CITED

Agnarsson I, May-Collado LJ. 2008. The phylogeny of Cetartiodactyla: the importance of dense taxon sampling, missing data, and the remarkable promise of cytocrome b to provide reliable species-level phylogenies. Mol Phylogenet Evol 48:964–985.

Allman JM, Hakeem A, Watson K. 2002. Two phylogenetic specializations in the human brain. Neuroscientist 8:335–346.

Allman JM, Watson KK, Tetreault NA, Hakeem AY. 2005. Intuition and autism: a possible role for Von Economo neurons. Trends Cogn Sci 9:367–373.

Allman JM, Tetreault NA, Hakeem AY, Kaufman JA, Manaye KF, Griffiths H, Semendeferi K, Erwin JM, Goubert V, Hof PR. 2009. The von Economo neurons in frontoinsular and anterior cingulate cortex in great apes and humans: a comparative and developmental study. Proc Natl Acad Sci U S A (in press).

Barbas H, Saha S, Rempel-Clower N, Ghashghaei T. 2003. Serial pathways from primate prefrontal cortex to autonomic areas may influence emotional expression. BMC Neurosci 4:25.

Behrmann G. 1993. Cytoarchitectonic studies of the cerebral cortex of the harbour porpoise, *Phocoena phocoena* (Linné, 1758). Invest Cetacea 24:261–285.

Berthoz S, Armony JL, Blair RJ, Dolan RJ. 2002. An fMRI study of intentional and unintentional (embarrassing) violations of social norms. Brain 125:1696–1708.

Bertrand I. 1930. Techniques histologiques de neuropathologie. Paris: Masson.

Boisserie JR, Lihoreau F, Brunet M. 2005. The position of Hippopotamidae within Cetartiodactyla. Proc Natl Acad Sci U S A 102:1537–1541.

Bromham L, Phillips MJ, Penny D. 1999. Growing up with dinosaurs: molecular dates and the mammalian radiation. Trends Ecol Evol 14: 113–118.

Cavada C, Company T, Tejedor J, Cruz-Rizzolo RJ, Reinoso-Suarez F. 2000. The anatomical connections of the macaque monkey orbitofrontal cortex. A review. Cereb Cortex 10:220–242.

Connor RC, Smolker RA, Richards AF. 1992. Two levels of alliance formation among male bottlenose dolphins (*Tursiops* sp.). Proc Natl Acad Sci U S A 89:987–990.

Craig AD. 2003. Interoception: the sense of the physiological condition of the body. Curr Opin Neurobiol 13:500–505.

Craig AD. 2004. Human feelings: why are some more aware than others? Trends Cogn Sci 8:239–241.

Craig AD. 2009. How do you feel—now? The anterior insula and human awareness. Nat Rev Neurosci 10: 59–70.

Craig AD, Reiman EM, Evans A, Bushnell MC. 1996. Functional imaging of an illusion of pain. Nature 384:258–260.

Eriksen N, Pakkenberg B. 2007. Total neocortical cell number in the mysticete brain. Anat Rec 290:83–95.

Fajardo C, Escobar MI, Buritica E, Arteaga G, Umbarila J, Casanova MF, Pimienta H. 2008. Von Economo neurons are present in the dorsolateral (dysgranular) prefrontal cortex of humans. Neurosci Lett 435:215–218.

Fordyce RE, Barnes LG. 1994. The evolutionary history of whales and dolphins. Annu Rev Earth Planet Sci 22:419–455.

Garey LJ, Leuba G. 1986. A quantitative study of neuronal and glial numerical density in the visual cortex of the bottlenose dolphin: evidence for a specialized subarea and changes with age. J Comp Neurol 247:491–496.

Gatesy J. 1997. More DNA support for a Cetacea/Hippopotamidae clade: the blood-clotting protein gene γ-fibrinogen. Mol Biol Evol 14:537–543.

Gingerich PD, Uhen MD. 1998. Likelihood estimation of the time of origin of cetacean and the time of divergence of cetacean and Artiodactyla. Paleo-Electronica 2:1–47.

Gingerich PD, Haq M, Zalmout IS, Khan IH, Malkani MS. 2001. Origin of whales from early artiodactyls: hands and feet of Eocene Protocetidae from Pakistan. Science 293:2239–2242.

Glezer II, Morgane PJ. 1990. Ultrastructure of synapses and golgi analysis of neurons in neocortex of the lateral gyrus (visual cortex) of the dolphin and pilot whale. Brain Res Bull 24:401–427.

Gundersen HJG. 1988. The nucleator. J Microsc 151:3–21.

Hakeem AY, Sherwood CC, Bonar CJ, Butti C, Hof PR, Allman JM. 2009. Von Economo neurons in the elephant brain. Anat Rec 292:242–248.

Haug H. 1987. Brain sizes, surfaces, and neuronal sizes of the cortex cerebri: a stereological investigation of man and his variability and a comparison with some mammals (primates, whales, marsupials, insectivores, and one elephant). Am J Anat 180:126–142.

Herman LM, Richards DG, Wolz JP. 1984. Comprehension of sentences by bottlenosed dolphins. Cognition 16:129–219.

Herman LM, Kuczaj S 2nd, Holder MD. 1993. Responses to anomalous gestural sequences by a language-trained dolphin: evidence for processing of semantic relations and syntactic information. J Exp Psychol 122:184–194.

Hof PR, Sherwood CC. 2005. Morphomolecular neuronal phenotypes in the neocortex reflect phylogenetic relationships among certain mammalian orders. Anat Rec 287:1153–1163.

Hof PR, Van der Gucht E. 2007. Structure of the cerebral cortex of the humpback whale, *Megaptera novaeangliae* (Cetacea, Mysticeti, Balaenopteridae). Anat Rec 290:1–31.

Hof PR, Nimchinsky EA, Young WG, Morrison JH. 2000. Numbers of Meynert and layer IVB cells in area V1: a stereologic analysis in young and aged macaque monkeys. J Comp Neurol 420:113–126.

Hof PR, Chanis R, Marino L. 2005. Cortical complexity in cetacean brains. Anat Rec 287:1142–1152.

Höistad M, Barbas H. 2008. Sequence of information processing for emotions through pathways linking temporal and insular cortices with the amygdala. NeuroImage 40:1016–1033.

Jacobs MS, Morgane PJ, McFarland WL. 1971. The anatomy of the brain of the bottlenose dolphin (*Tursiops truncatus*). Rhinic lobe (rhinencephalon). I. The paleocortex. J Comp Neurol 141:205–271.

Jacobs MS, McFarland WL, Morgane PJ. 1979. The anatomy of the brain of the bottlenose dolphin (*Tursiops truncatus*). Rhinic lobe (Rhinencephalon): The archicortex. Brain Res Bull 4(Suppl 1):1–108.

Jacobs MS, Galaburda AM, McFarland WL, Morgane PJ. 1984. The insular formations of the dolphin brain: quantitative cytoarchitectonic studies of the insular component of the limbic lobe. J Comp Neurol 225:396–432.

Jerison HJ. 1973. Evolution of the brain and intelligence. New York: Academic Press.

Kaufman JA, Paul LK, Manaye KF, Granstedt AE, Hof PR, Hakeem AY, Allman JM. 2008. Selective reduction of Von Economo neuron number in agenesis of the corpus callosum. Acta Neuropathol 116:479–489.

Kraus C, Pilleri G. 1969. Quantitative Untersuchungen über die Großhirnrinde des Cetaceen. Invest Cetacea 1:127–150.

Krushinskaya NL. 1986. The behaviour of cetaceans. Invest Cetacea 19: 115–273.

Krutzen M, Mann J, Heithaus MR, Connor RC, Bejder L, Sherwin WB. 2005. Cultural transmission of tool use in bottlenose dolphins. Proc Natl Acad Sci U S A 102:8939–8943.

Kumar S, Hedges SB. 1998. A molecular timescale for vertebrate evolution. Nature 392:917–920.

Lusseau D. 2007. Evidence for social role in a dolphin social network. Evol Ecol 21:357–366.

Manger PR. 2006. An examination of cetacean brain structure with a novel hypothesis correlating thermogenesis to the evolution of a big brain. Biol Rev 81:293–338.

Manger P, Sum M, Szymanski M, Ridgway S, Krubitzer L. 1998. Modular subdivisions of dolphin insular cortex: does evolutionary history repeat itself? J Cogn Neurosci 10:153–166.

Marino L. 1998. A comparison of encephalization between odontocete cetaceans and anthropoid primates. Brain Behav Evol 51:230–238.

Marino L. 2002. Convergence of complex cognitive abilities in cetaceans and primates. Brain Behav Evol 59:21–32.

Marino L. 2007. Cetacean brains: how aquatic are they? Anat Rec 290: 694–700.

Marino L, McShea DW, Uhen MD. 2004. Origin and evolution of large brains in toothed whales. Anat Rec 281:1247–1255.

Marino L, Connor RC, Fordyce RE, Herman LM, Hof PR, Lefebvre L, Lusseau D, McCowan B, Nimchinsky EA, Pack AA, Rendell L, Reidenberg JS, Reiss D, Uhen MD, Van der Gucht E, Whitehead H. 2007. Cetaceans have complex brains for complex cognition. PLoS Biol 5:e139.

Marino L, Butti C, Connor RC, Fordyce RE, Herman LM, Hof PR, Lefebvre L, Lusseau D, McCowan B, Nimchinsky EA, Pack AA, Reidenberg JS, Reiss D, Rendell L, Uhen MD, Van der Gucht E, Whitehead H. 2008. A claim in search of evidence: reply to Manger's thermogenesis hypothesis of cetacean brain structure. Biol Rev 83:417–440.

Morgane PJ, Jacobs MS, McFarland WL. 1980. The anatomy of the brain of the bottlenose dolphin (*Tursiops truncatus*). Surface configurations of the telencephalon of the bottlenose dolphin with comparative anatomical observations in four other cetacean species. Brain Res Bull 5(Suppl 3):1–107.

Morgane PJ, McFarland WL, Jacobs MS. 1982. The limbic lobe of the dolphin brain: a quantitative cytoarchitectonic study. J Hirnforsch 23: 465–552.

Morgane PJ, Glezer II, Jacobs MS. 1988. Visual cortex of the dolphin: an image analysis study. J Comp Neurol 273:3–25.

Nimchinsky EA, Vogt BA, Morrison JH, Hof PR. 1995. Spindle neurons of the human anterior cingulate cortex. J Comp Neurol 355:27–37.

Nimchinsky EA, Gilissen E, Allman JM, Perl DP, Erwin JM, Hof PR. 1999. A neuronal morphologic type unique to humans and great apes. Proc Natl Acad Sci U S A 96:5268–5273.

Oelschläger HA, Oelschläger JS. 2002. Brains. In: Perrin WF, Würsig B, Thewissen JGM, editors. Encyclopedia of marine mammals. San Diego: Academic Press. p 133–158.

Ongür D, Price JL. 2000. The organization of networks within the orbital and medial prefrontal cortex of rats, monkeys and humans. Cereb Cortex 10:206–219.

Plotnik JM, de Waal FBM, Reiss D. 2006. Self-recognition in an Asian elephant. Proc Natl Acad Sci U S A 103:17053–17057.

Poole JH, Moss CJ. 2008. Elephant sociality and complexity; The scientific evidence. In: Wemmer C, Christen K, editors. Never forgetting; elephants and ethics. Baltimore: Johns Hopkins University Press.

Poth C, Fung C, Güntürkün O, Ridgway SH, Oelschläger HHA. 2005. Neuron numbers in sensory cortices of delphinids compared with a physeterid, the pygmy sperm whale. Brain Res Bull 66:357–360.

Rainville P, Duncan GH, Price DD, Carrier B, Bushnell MC. 1997. Pain affect encoded in human anterior cingulate but not somatosensory cortex. Science 277:968–971.

Reiss D, Marino L. 2001. Mirror self-recognition in the bottlenose dolphin: a case of cognitive convergence. Proc Natl Acad Sci U S A 98:5937–5942.

Rivara CB, Sherwood CC, Bouras C, Hof PR. 2003. Stereologic characterization and spatial distribution patterns of Betz cells in the human primary motor cortex. Anat Rec 270:137–151.

Schmitz C, Hof PR. 2005. Design-based stereology in neuroscience. Neuroscience 130:813–831.

Schmitz C, Dafotakis M, Heinsen H, Mugrauer K, Niesel A, Popken GJ, Stephan M, Van de Berg WD, von Hörsten S, Korr H. 2000. Use of cryostat sections from snap-frozen nervous tissue for combining stereological estimates with histological, cellular, or molecular analyses on adjacent sections. J Chem Neuroanat 20:21–29.

Schmitz C, Grolms N, Hof PR, Boehringer R, Glaser J, Korr H. 2002. Altered spatial arrangement of layer V pyramidal cells in the mouse brain following prenatal low-dose X-irradiation. A stereological study using a novel three-dimensional analysis method to estimate the nearest neighbor distance distributions of cells in thick sections. Cereb Cortex 12:954–960.

Schwerdtfeger WK, Oelschläger HA, Stephan H. 1984. Quantitative neuroanatomy of the brain of the La Plata dolphin, *Pontoporia blainvillei*. Anat Embryol 170:11–19.

Seeley WW, Carlin DA, Allman JM, Macedo MN, Bush C, Miller BL, Dearmond SJ. 2006. Early frontotemporal dementia targets neurons unique to apes and humans. Ann Neurol 60:660–667.

Seeley WW, Allman JM, Carlin DA, Crawford RK, Macedo MN, Greicius MD, Dearmond SJ, Miller BL. 2007. Divergent social functioning in behavioral variant frontotemporal dementia and Alzheimer disease: reciprocal networks and neuronal evolution. Alzheimer Dis Assoc Disord 21:S50–S57.

Sherwood CC, Lee PWH, Rivara CB, Holloway RL, Gilissen EPE, Simmons RMT, Hakeem A, Allman JM, Erwin JM, Hof PR. 2003. Evolution of specialized pyramidal neurons in primate visual and motor cortex. Brain Behav Evol 61:28–44.

Shin LM, Dougherty DD, Orr SP, Pitman RK, Lasko M, Macklin ML, Alpert NM, Fischman AJ, Rauch SL. 2000. Activation of anterior paralimbic structures during guilt-related script-driven imagery. Biol Psychiatry 48:43–50.

Singer T, Seymour B, O'Doherty J, Kaube H, Dolan RJ, Frith CD. 2004. Empathy for pain involves the affective but not sensory components of pain. Science 303:1157–1162.

Tandrup T, Gundersen HJG, Jensen EB. 1997. The optical rotator. J Microsc 186:108–120.

Tower DB. 1954. Structural and functional rganization of mammalian cerebral cortex: the correlation of neurone density with brain size. Cortical neurone density in the fin whale (*Balaenoptera physalus* L.) with a note on the Indian elephant. J Comp Neurol 101:19–51.

Von Economo C. 1926. Eine neue Art Spezialzellen des Lobus cinguli und Lobus insulae. Z Ges Neurol Psychiatr 100:706–712.

Wang SS, Shultz JR, Burish MJ, Harrison KH, Hof PR, Towns LC, Wagers MW, Wyatt KD. 2008. Functional trade-offs in white matter axonal scaling. J Neurosci 28:4047–4056.

Watson KK, Jones TK, Allman JM. 2006. Dendritic architecture of the von Economo neurons. Neuroscience 141:1107–1112.

West MJ, Slomianka L, Gundersen HJG. 1991. Unbiased stereological estimation of the total number of neurons in the subdivisions of the rat hippocampus using the optical fractionator. Anat Rec 231:482–497.